Production of birnessite-type manganese oxides by biofilms from oxygen-supplemented biological activated carbon (BAC) filters

Larasati, Amanda; Bernadet, Olga; Euverink, Gert Jan W.; van Veelen, H. Pieter J.; Gagliano, Maria Cristina

Published in:
Environmental Science: Water Research and Technology

DOI:
10.1039/d4ew00208c

Environmental Science
Water Research & Technology

ROYAL SOCIETY OF CHEMISTRY

PAPER

View Article Online
View Journal | View Issue

Cite this: *Environ. Sci.: Water Res. Technol.*, 2024, **10**, 2844

Production of birnessite-type manganese oxides by biofilms from oxygen-supplemented biological activated carbon (BAC) filters†

Amanda Larasati, ‡[a] Olga Bernadet, ‡[ab] Gert Jan W. Euverink, [b] H. Pieter J. van Veelen [a] and Maria Cristina Gagliano *[a]

Received 15th March 2024,
Accepted 19th August 2024

DOI: 10.1039/d4ew00208c

rsc.li/es-water

Biological oxidation of manganese (Mn) by bacteria results in the formation of biogenic Mn oxides (MnOx), which are known to be strong oxidants and effective catalysts. Manganese-oxidizing bacteria (MnOB) often develop in engineered systems for water treatment under oligotrophic conditions. In this study, we investigated the MnOB within biofilms sampled in two different seasons from full-scale oxygen-supplemented biological activated carbon (BAC) filters performing the complete removal of Mn from wastewater. By applying a novel batch enrichment approach ensuring the continuous presence of soluble Mn, after 42 days the start-up microbial community grew into thick, floccular biofilms efficiently oxidizing Mn^{2+} into numerous black nodules. The amount of Mn oxidized was quantified using inductively coupled plasma optical emission spectroscopy (ICP-OES). X-ray diffraction (XRD) analysis and scanning electron microscopy (SEM) revealed that the MnOx formed was a birnessite-type (δ-MnO_2) with a crystalline, nanoflower structure. Comparison of the microbial community composition before and after the enrichment by means of 16S rRNA gene amplicon sequencing showed increases of members of the orders *Rhizobiales* and *Burkholderiales*, and identified among the most abundant some bacterial groups which have rarely or never been associated with Mn oxidation before (*Rhodococcus*, *Ellin6067*, *Planctomycetota* Pir4 lineage, *Rhizobiales* A0839 and Amb-16S-1323). This study unravels the potential of production of crystalline MnOx by mixed-microbial communities which uniquely generate in a man-made biofilter. The new insights provided implement the knowledge in the field, with the perspective to design innovative biotechnologies to remove recalcitrant compounds where MnOB find optimal growth conditions to produce catalytic forms of MnOx.

Water impact

Manganese-oxidizing bacteria (MnOB) often develop in biofilters for water treatment under oligotrophic conditions. Herein, by applying a novel enrichment approach, we used biofilms from full-scale biological activated carbon filters to synthesize nanoflower-shaped birnessite crystals. As birnessite-type Mn oxides are effective catalysts for water remediation, we highlight the potential of MnOB enriched-communities to improve the removal of recalcitrant organics in biotechnological contexts.

1 Introduction

Manganese (Mn) is the second most abundant transition element on earth after iron,[1] occurring naturally in groundwater, surface water, freshwater, and seawater, mostly in the Mn^{2+} soluble form.[2] In the presence of oxidants (abiotic or biotic) and changes in pH, Mn^{2+} is oxidized to insoluble Mn^{3+}, Mn^{4+}, or a higher oxidation state, depending on the oxidant,[3] forming Mn oxides (MnOx). In aquatic environments, Mn^{2+} abiotic oxidation by O_2 is not favored at pH below 8 due to the high activation energy,[4] requiring an alternative oxidant such as mineral surfaces.[5] In contrast, biogenic Mn^{2+} oxidation by bacteria, fungi, or algae is generally 4–5 orders of magnitude faster than the abiotic one.[6] The majority of naturally occurring MnOx are believed to be derived from biogenic Mn^{2+} oxidation,[7] and biogenic MnOx are among the strongest natural oxidizing agents.[8]

[a] *Wetsus, European Centre of Excellence for Sustainable Water Technology, Oostergoweg 9, 8911 MA, Leeuwarden, The Netherlands. E-mail: cristina.gagliano@wetsus.nl; Tel: +31582843013*
[b] *Engineering and Technology Institute Groningen (ENTEG), University of Groningen, Nijenborgh 4, Groningen, The Netherlands*

† Electronic supplementary information (ESI) available. See DOI: https://doi.org/10.1039/d4ew00208c

‡ Amanda Larasati and Olga Bernadet contributed equally to this article.

Among manganese-oxidizing microorganisms, manganese-oxidizing bacteria (MnOB) consist of numerous species with a wide phylogenetic distribution.[3,9] Several bacterial isolates were classified as MnOB, belonging to 4 phyla, namely *Actinobacteriota*, *Bacteroidota*, *Firmicutes*, and *Proteobacteria*.[9–11] Two main hypotheses have been proposed to explain why bacteria oxidize Mn^{2+}: (i) the properties of MnOx (adsorption, cation exchange, and redox functionality) provide them protection from oxidative stress, heavy metal toxicity, and UV radiation, and aid in the biodegradation of recalcitrant organics;[9,11] (ii) Mn oxidation can be coupled with adenosine triphosphate (ATP) synthesis, promoting autotrophic bacterial growth *via* chemolithoautotrophy in oligotrophic environments, with Mn^{2+} as the sole energy source (*e.g.*, ref. 12 and 13). A major fraction of biogenic MnOx is indeed produced under oligotrophic conditions,[9] thus communities rich in MnOB often develop in water treatment processes[14,15] or drinking water facilities,[16,17] where such conditions prevail. Mn^{2+} is often efficiently removed through granular media biofiltration, where MnOB grow as biofilms on filtration media (*i.e.*, activated carbon, sand) converting Mn^{2+} into black, insoluble MnOx particles.[14,18,19] The negatively charged extracellular polymeric substance (EPS) of the biofilm matrix facilitates sorption and biological oxidation of metals.[20,21] In biological activated carbon (BAC) systems, Mn^{2+} is adsorbed in the biofilm and oxidized by the extracellular enzymes of MnOB[8,10] to form particulate oxides[14] that may be removed by backwashing[22] unless associated with the carbon granule surface.[23] Due to their oxidation and adsorption properties, biogenic MnOx can theoretically catalyze the transformation of a wide range of organics and remove metals.[1,11] Based on this, synthetic MnOx-coated filtration media have been already applied for the removal of several contaminants.[24,25] A biological filtration process, in which MnOx are naturally enriched within biofilms, can be an added value for wastewater treatment towards enhancing water reuse. Recently, biofiltration research has focused on tailoring microbial community development to improve its performance.[26] Several studies have investigated the microbial communities in BAC filter biofilms (*e.g.*, ref. 27–29), and recently, much attention was devoted to the Mn-oxidizing sub-populations in full-scale biofilters for the production of drinking water from surface/groundwater sources.[22,23,30,31] However, thorough investigations on Mn removing communities in full-scale biofilters connected to wastewater reuse treatment plants are lacking. In our previous research, we characterized the process performances of full-scale, oxygen augmented BAC filters (service life 11 years) within the UPW factory (Emmen, NL), a successful example of a wastewater reuse technology, where the secondary effluent of a wastewater treatment plant (WWTP) is treated to produce ultrapure water.[32] The BAC filters of the UPW factory operated the complete removal of Mn from wastewater over 2-year monitoring.[33,34] Mn-oxide particles were visualized within the BAC biofilms washed out during every backwashing cycle.[33] The aim of this research was to shed light on the importance and predominance of biological Mn removal in this unique oxygen augmented biofiltration system treating wastewater. In this multidisciplinary study, a novel approach was applied for the culture of the MnOB from BAC biofilms collected from the UPW factory, feeding manganese carbonate ($MnCO_3$) as the sole medium component, thus ensuring their enrichment under batch conditions with the continuous presence of Mn^{2+} in water as in the full-scale filters, without the need for medium replacement. The results showed that, under the applied oligotrophic conditions, most of the soluble Mn^{2+} was oxidized, a source of energy for the extensive growth of biofilms. Within the biofilms, a large amount of crystalline MnOx, mostly identified as birnessite, was synthesized by a core microbiome of bacteria belonging to the orders *Burkholderiales* and *Rhizobiales* originating from different natural environments.

Due to their catalytic activity, the formation of highly crystalline MnOx products by the collaboration of phylogenetically distinct bacteria that naturally live in diverse environments is unique potential of man-made biofilters which deserves more research. This is in opposition to the formation of poorly crystalline MnOx (with low catalytic activity) which can also happen in biofilters and likely proceeds without direct control by the microorganism.[35] Thus, the findings generated in this study represent new biological insights into the potential of mixed microbial cultures to form complex MnOx structures, with the perspective to stimulate the selective growth of these natural Mn-removing microbial communities within existing treatment plants for different biotechnological applications.

2 Materials and methods

2.1 Inoculum source

The inoculum biofilm samples to prepare the enrichment cultures were obtained from the BAC filters of a plant producing ultrapure water (UPW factory, Emmen, NL) from secondary wastewater treatment effluent. A description of the UPW factory is reported in the ESI† (Fig. S1). These BAC filters are operated with periodic pure-oxygen dosing to maintain full aerobic conditions[32] (reaching concentrations up to 40 mg L^{-1} (ref. 34)) and always achieve high Mn removal.[33] The biofilms were harvested from the backwash water during the periodic backwashing of BAC filters with air and water. Backwash water was collected in acid-washed LDPE bottles from the top of the filters within the first 5 min after the backwashing started and was stored at 4 °C. The samples are referred to as "inoculum biofilm" (IB) hereafter. Two different samplings were executed in two different seasons, in September 2021 and January 2022, before and after the BAC filters maintenance (October 2021) with 7 days of inoperability. The composition of the water containing the IB is reported in Table S1.†

2.2 Preparation of Mn enrichment cultures

To prepare enrichment cultures of MnOB, 100 mL of the IBs collected in September 2021 and January 2022 were placed into 100 mL borosilicate glass bottles with inside walls coated with manganese carbonate ($MnCO_3$ (Alfa Aesar, US)) slurry as a source of soluble Mn^{2+}, with a final concentration of ~20 mM, and dried overnight in the dark.[13] $MnCO_3$ (Mn^{2+}-bearing carbonate) was used to enable long-term enrichment. $MnCO_3$ has low solubility in water, is sensitive to redox changes,[36] and can be oxidized by microorganisms.[37,38] This ensured the continuous presence of Mn^{2+} in water at neutral pH and room temperature, allowing continuous enrichment without the need for medium replacement. To assess if the Mn oxidation was related to biological activity, control bottles were prepared with IB samples inactivated by autoclaving (121 °C, 103 kPa, 20 min). These are referred to as non-active biofilms hereafter. All experiments were run in triplicate per condition (active and non-active biofilms) and per sampling events (September (Sept) and January (Jan)). The bottles were closed with gauze cloth to ensure air exchange and incubated at room temperature in the dark for 42 days. Samples were analyzed before and after the incubation, as described in the following sections. Water evaporation of 10% after the 42-day experiment was considered.

2.3 Characterization of biofilms and Mn oxides

2.3.1 Volatile suspended solid (VSS) and pH measurement. The biomass growth in the biofilm cultures was monitored by measuring the VSS before and after the experiment, using the standard protocol EPA 160.4.[39] The pH during the experiment was measured using a SevenExcellence pH meter S470 (Mettler Toledo®, CH).

2.3.2 Optical microscopy and biofilm staining. Biofilm aggregates from experimental bottles were analyzed on glass slides using optical microscopy (DM750, Leica, DE), and images were acquired using Leica LAS-X v4.12 software. Extracellular polymeric substances (EPSs) of biofilms were visualized by mixing 100 µl of the sample with 20 µl of 0.1% crystal violet, targeting proteins and polysaccharides.[40]

2.3.3 Scanning electron microscopy (SEM) and energy dispersive X-ray spectroscopy (EDX). The $MnCO_3$ slurry and all the biofilm samples were visualized through SEM analysis. Sample preparation followed the protocol described by Bernadet *et al.*[33] and was modified according to Yu and Leadbetter,[41] with fixation in 2.5% glutaraldehyde, washing with 25 mM HEPES buffer at pH 7.5, dehydration with ethanol, and a final dehydration step with critical point drying (EM CPD3000, Leica, DE), where ethanol was replaced with liquid CO_2 at <10 °C and 55 bar. SEM imaging was performed on the dried samples using a JSM-6480LV (JEOL, JP) at an operating voltage of 6 kV. Elemental analysis was carried out through EDX with an x-act SSD-EDX detector (Oxford Instruments, UK) coupled with SEM imaging at an acceleration voltage of 15 kV.

2.3.4 Inductively coupled plasma optical emission spectroscopy (ICP-OES). The Mn concentration in the IB and at the end of the experiment for the active and non-active biofilms was measured on unfiltered samples using an Optima 5300 DV ICP-OES (Perkin Elmer, US) with argon as carrier gas, after addition of nitric acid (HNO_3) (2% final concentration). Since biological Mn oxidation converts soluble Mn^{2+} into insoluble MnOx (Mn^{3+} and Mn^{4+}), the Mn concentration was classified, on the basis of Mn solubility in HNO_3, as "acid-soluble" and 'acid-insoluble" fractions, as described previously.[41] For the method development and assessment, four Mn salts were used as references based on their Mn oxidation state and the solubility of the Mn species in HNO_3 (Table S2 and ESI†). The procedure for measuring Mn fractions in both reference and experimental samples was as follows: 4.5 mL of sample and 0.5 mL of 69% HNO_3 (VWR, US) were put inside a centrifuge tube. The tube was mixed in the dark overnight (~15 h) to reassure that all the Mn^{2+} was in the soluble state. 1 mL of the sample was measured using ICP-OES and is called the "acid-soluble fraction". 2 mL of the sample was further mixed with 4.8 mL of 69% HNO_3 and 4 mL 30% H_2O_2 (VWR, US) and subjected to microwave-assisted digestion (Ethos Easy, Milestone SRL, IT) at 180 °C for 30 min in isothermal mode. The sample was then diluted until it contained 2% of HNO_3 and measured by ICP-OES as the "total Mn". The "acid-insoluble fraction" was derived by subtracting the "acid-soluble fraction" from "total Mn".

2.3.5 X-ray diffraction (XRD) analysis. Phase identification of MnOx particles generated in the Sept and Jan bottles was carried out on freeze dried samples with powder XRD, using a diffractometer (D8 advance, Bruker, GR) with Cu Kα radiation (30 kV, 30 mA, λ = 1.034 Å). A low background silicon sample holder was used during the analysis. The obtained XRD patterns were compared with the Crystallography Open Database (COD, **https://www.crystallography.net/cod/**) using Mn as the mandatory element to determine the mineral phases of samples.

2.4 Microbial community analysis

Microbial community analysis based on next generation sequencing (NGS) of 16S rRNA gene amplicons was performed on the IB samples and the enrichment cultures after 42 days. 10 mL of culture from two replicate experimental bottles was centrifuged at 4750*g* at 4 °C for 5 min. The liquid was decanted, and the pellet was washed with PBS and used for DNA extraction with the FastDNA™ Spin kit for soil (MP Biomedicals, US), following the manufacturer's instructions. The extracted DNA was quantified using fluorescence spectroscopy (QuantiFluor dsDNA system and Quantus™ fluorometer (Promega, US)). The V4–V5 region of the 16S rRNA gene of bacteria was amplified using PCR primers 515F[42] and 926R.[43] Amplicon sequencing was performed with 2 × 300 bp (V3) paired-end sequencing on a MiSeq (Illumina, US) at MR DNA (Molecular Research LP) (Shallowater, US). Negative extraction and mock community controls were included. Quality control of sequences was performed in QIIME2 (v. 2019.10),[44] where DADA2 (ref. 45) was used for error correction and inference of exact amplicon sequence variants (ASVs). Taxonomic classification of ASVs was based on the SILVA

v.138.1 database.[46] A total of 2562 ASVs were detected, and a coverage of on average (range) 62 347 (48 342, 71 242) sequences per sample captured the microbial diversity of the samples (Fig. S2†). The sample by the ASV frequency matrix was rarefied (mean of 100 iterations) at 48 342 sequences per sample and agglomerated at the genus level. The genus relative abundances and alpha diversity (Shannon) were calculated. Beta diversity visualized compositional differences among the bottles applying principal coordinate analysis of Bray–Curtis dissimilarities, an ecological metric of compositional difference. QIIME2 scripts and an Rmarkdown document for the analyses are accessible from Github (**https://github.com/pietervanveelen/Larasati_Mn_oxidation_16SrRNA**). Sequencing data were deposited in the European Nucleotide Archive (ENA), project number PRJEB64232.

3 Results and discussion

3.1 Biomass growth and Mn nodules were observed in the active cultures

After 42 days, the difference between non-active and active biofilms was clearly visible, with control bottles retaining the light-brown color of $MnCO_3$ slurry (Fig. 1a), while all the cultures fed with active IBs turned dark brown to black (Fig. 1d). A closer look at the active biofilms using microscopy showed the presence of floccular biofilms with a robust EPS matrix extensively loaded with black nodules (Fig. 1e and f), opposite to the non-active biofilms, where unconverted $MnCO_3$ was still visible (Fig. 1b and c). Similar black MnOx nodules from biological oxidation were previously observed microscopically under laboratory conditions.[13,47] Further visual analysis by SEM and EDX showed that the raw $MnCO_3$ slurry particles (Fig. 2a and S3A†) covered the non-active biofilms (Fig. 2b and S3B†), confirming the lack of conversion into nodules. Conversely, in both Sept and Jan bottles the aggregates in active biofilms (Fig. 2c and e) mostly contained Mn in the form of crystals with nanoflower structures, clearly distinguishable by shape in comparison with the raw $MnCO_3$ particles (Fig. 2d and f). EDX analysis confirmed that these structures were rich in Mn (Fig. S3C and D†). Most MnOx formed through biological oxidation in the environment were found to have a 3D flower-like layered structure, such as buserite and birnessite (δ-MnO_2).[48] It is worth noting that the active biofilms originating from the Sept IB showed a higher presence of nanoflower structures (Fig. 2c) than the bottles inoculated with the Jan IB, in which more unconverted $MnCO_3$ particles were visible (Fig. 2e).

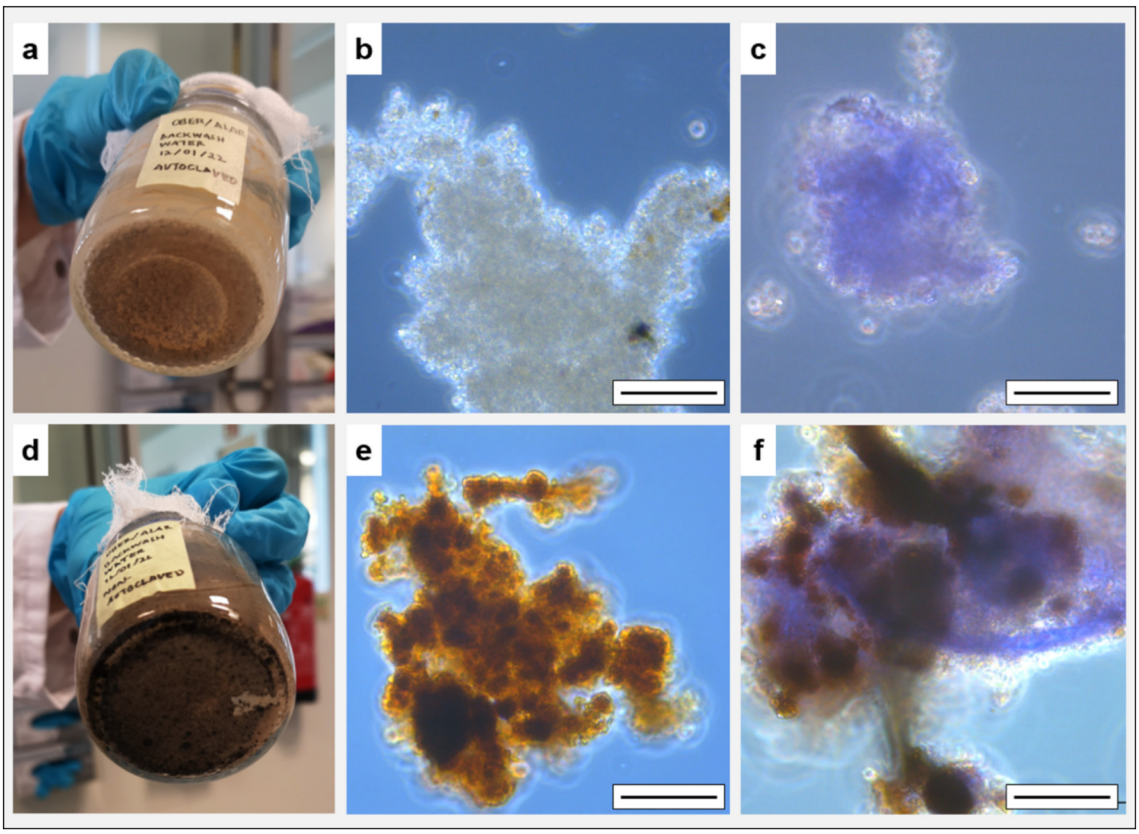

Fig. 1 – Representative photos and micrographs showing the difference between non-active (control) and active biofilms after 42 days of incubation with $MnCO_3$. Bottles with non-active biofilms preserved the light-brown color of $MnCO_3$ slurry (a), and microscopy observation showed the persistence of $MnCO_3$ as salt (b) and the original EPS matrix (c). Bottles inoculated with active biofilms were dark brown to black (d), and the biofilm grown accumulated black nodules (e) and EPSs (visualized after crystal violet staining) (f). Scale bars are 20 μm.

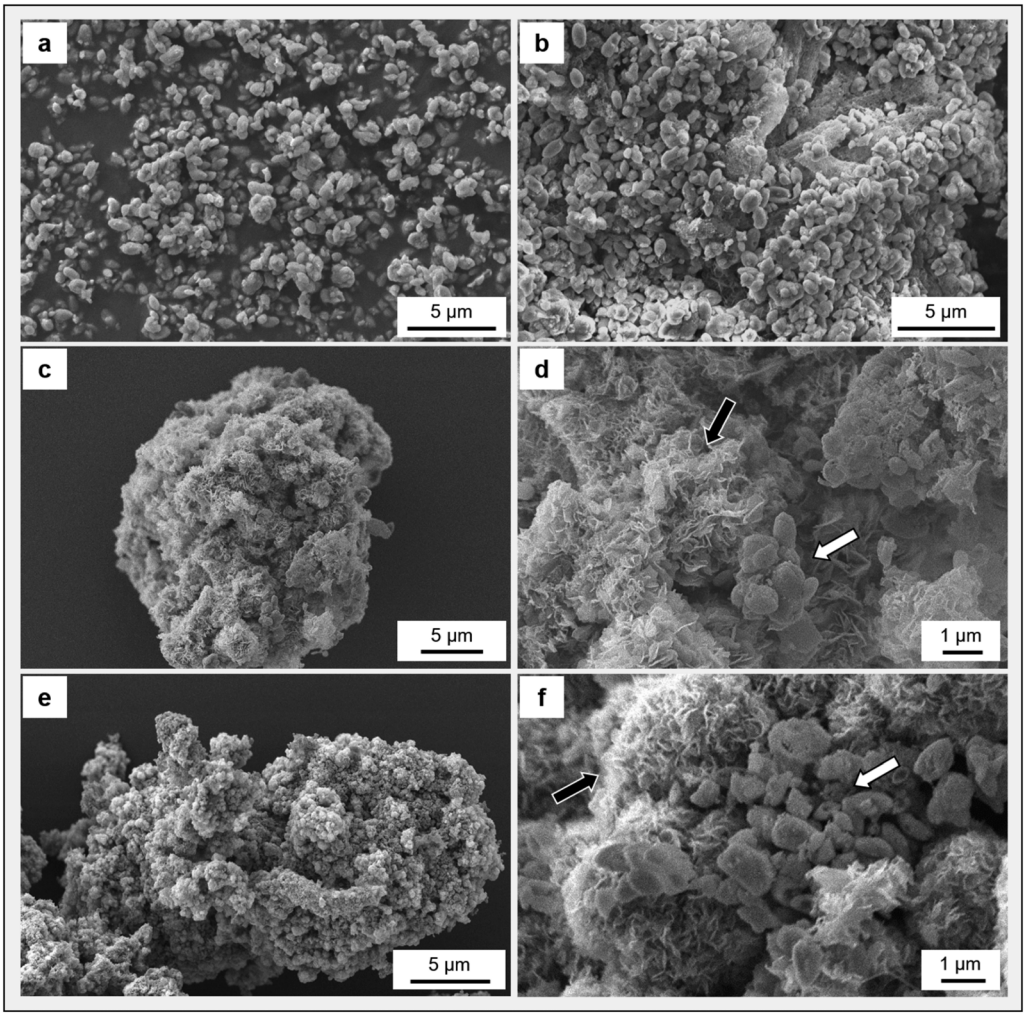

Fig. 2 – Scanning electron microscopy (SEM) images of samples taken before and after the 42-day experiment. The $MnCO_3$ slurry alone was composed of small, tightly aggregated round particles (a). In (b), the non-active biofilm (control) at the end of the experiment was covered with $MnCO_3$ particles. After 42 days, in active biofilms from Sept (c and d) and Jan (e and f) bottles the $MnCO_3$ particles (white arrows) were converted into Mn oxide crystals with a nanoflower structure (black arrows).

This could be a consequence of maintenance procedures to the BAC filters preceding the sampling of January 2022, which left the BAC granules without nutrients and minerals for 7 days, potentially affecting the microbial community. Based on VSS measurements, active biofilms developed over time from the start-up IB, while control, non-active biofilms remained stable (Table 1). Assuming that the growth is only related to either heterotrophic utilization of the organics present in the initial water samples (89 and 56 mg L^{-1} expressed as total chemical oxygen demand (tCOD) for the Sept and Jan samples, respectively) (Table S1†) or autotrophic consumption of (bi)carbonate ions from $MnCO_3$,[3] VSS values for both experiments were relatively high compared to BAC biofilms growing under similar oligotrophic experimental conditions.[49,50]

Thus, these results collectively support the hypothesis that the oxidation of Mn^{2+} was providing energy for growth, being the sole energy source for some bacteria when oxidation is coupled with ATP synthesis *via* chemolithoautotrophy, as discovered in early studies on single strains from oligotrophic environments.[51–53] Biological Mn^{2+} oxidation with various electron acceptors can provide energy for microorganisms, but it is not thermodynamically favored at low pH.[54] The pH values in all bottles at the end of the experiments were around neutral, with a slightly higher pH

Table 1 – Volatile suspended solids (VSSs) and pH values measured in duplicate on the start-up inoculum biofilm, in comparison with the non-active (control) and active enrichment cultures after 42 days. For each experiment (Sept and Jan), mean values ± standard deviations were calculated on triplicate bottles

Experiment	Sample	VSS (mg L^{-1})	pH
Sept	Inoculum biofilm	51 ± 1.0	7.9 ± 0.01
	Non-active biofilm	55 ± 24	8.2 ± 0.05
	Active biofilm	255 ± 7.1	7.4 ± 0.07
Jan	Inoculum biofilm	23 ± 1.0	7.3 ± 0.01
	Non-active biofilm	58 ± 29	7.8 ± 0.09
	Active biofilm	410 ± 96	7.4 ± 0.01

Table 2 – Mn^{2+}oxidation trends analyzed with ICP-OES in the IB compared to non-active (control) and active biofilms after 42 days of enrichment with $MnCO_3$ for the Sept and Jan experiments. The amounts of soluble Mn^{2+} and insoluble MnOx (Mn^{3+} and Mn^{4+}) are called "acid-soluble" and "acid-insoluble" fractions, respectively. The "acid-insoluble" fraction was calculated as the difference between the "total Mn" and "acid-soluble" fraction. For each experiment (Sept and Jan), mean values ± standard deviations were calculated on triplicate bottles

		Mn concentration (mmol L^{-1})			Mn fraction (%)	
Experiment	Sample	Total	Acid-soluble	Acid-insoluble	Acid-soluble	Acid-insoluble
Sept	Inoculum biofilm	0.1 ± 0.003	0.1 ± 0.004	0.01 ± 0.005	93.7% ± 4.5%	6.3% ± 4.6%
	Non-active biofilm	22.4 ± 0.8	20.6 ± 1.2	1.8 ± 1.4	91.9% ± 6.2%	8.1% ± 6.3%
	Active biofilm	22.4 ± 0.3	3.4 ± 0.2	19 ± 0.4	15.2% ± 0.8%	84.8% ± 2.1%
Jan	Inoculum biofilm	0.04 ± 0.002	0.034 ± 0.003	0.003 ± 0.003	92.9% ± 8.9%	7.1% ± 9.2%
	Non-active biofilm	20.6 ± 0.7	18.9 ± 0.5	1.6 ± 0.9	92.3% ± 4.1%	7.7% ± 4.3%
	Active biofilm	20.3 ± 0.5	9.7 ± 0.1	10.6 ± 0.5	47.9% ± 1.3%	52.1% ± 2.7%

in the control cultures (Table 1). Moreover, under the experimental conditions applied (atmospheric pressure and 20% O_2 from air) and at a pH below 8, the abiotic Mn^{2+} oxidation is not favored since a high activation energy is required for oxidation by O_2,[55] as also depicted in the adapted Pourbaix diagram in Fig. S4.†

3.2 Characterization of the conversion of soluble into insoluble Mn

To determine the fraction of soluble Mn^{2+} added as $MnCO_3$ into the experimental bottles that was converted into insoluble Mn^{3+} and/or Mn^{4+}, a dedicated method was developed applying ICP-OES to determine Mn concentrations as "acid-soluble" and 'acid-insoluble" fractions (section 2.3.2). At the end of the 42-day experiment, the bottles with non-active and active biofilms contained the same amount of total Mn, while the amount of acid-insoluble Mn (Mn^{3+} and/or Mn^{4+}) was 6- to 10-fold higher for the active biofilms (Table 2), further supporting the biological Mn oxidation. The fractions of acid-soluble (the unconverted Mn^{2+}) and insoluble Mn present in the non-active biofilm samples were similar to those in the IB, indicating that the abiotic oxidation did not occur even though the water pH values were higher (7.8–8.2) than in the active biofilm bottles (7.4) (Table 1). Active biofilms converted most of the soluble Mn^{2+} to acid-insoluble forms, and the converted fraction in the active biofilm of Sept bottles was higher (average of 84.8%) than in the Jan ones (average of 52.1%) (Table 2). Differences in the oxidation of Mn between the Sept and Jan samples were also observed by XRD analysis (Fig. 3). The XRD patterns of the active biofilms in the Sept experiment identified the produced MnOx as birnessite-type (or δ-MnO_2), based on the COD database (COD 9013652 (ref. 56)), referring to the two distinctive peaks from the 00 *l* reflections at 12.01° 2θ (λ = 7.36 Å) and 24.16° 2θ (3.68 Å) (Fig. 3a). Another two peaks appearing at 36.9° 2θ (2.43 Å) and 66.2° 2θ (1.4 Å) are indexed to birnessite, which are broad and have low signal-to-noise ratios, likely corresponding to small sized crystals[57] (Fig. 3a). δ-MnO_2 is defined as a layered polymorph with repeating single layers of MnO_2, separated by cations and/or water molecules.[58] Interestingly, the XRD patterns of the biologically formed MnOx in the Sept experiment were similar to abiotically synthesized H^+-birnessite or H^+ inserted between layers.[35] Their morphology (Fig. 2d) was also similar to δ-MnO_2 chemically synthesized using potassium permanganate ($KMnO_4$) and hydrochloric acid (HCl), where the oxide structure is built-up of nanosheets, forming nanoflower structures.[59]

Synthetic birnessite-type δ-MnO_2 with a nanoflower morphology exhibits excellent ability to remove various chemical species,[60,61] showing higher oxidation activity than other morphologies, such as nanosheets or nanowires.[62]

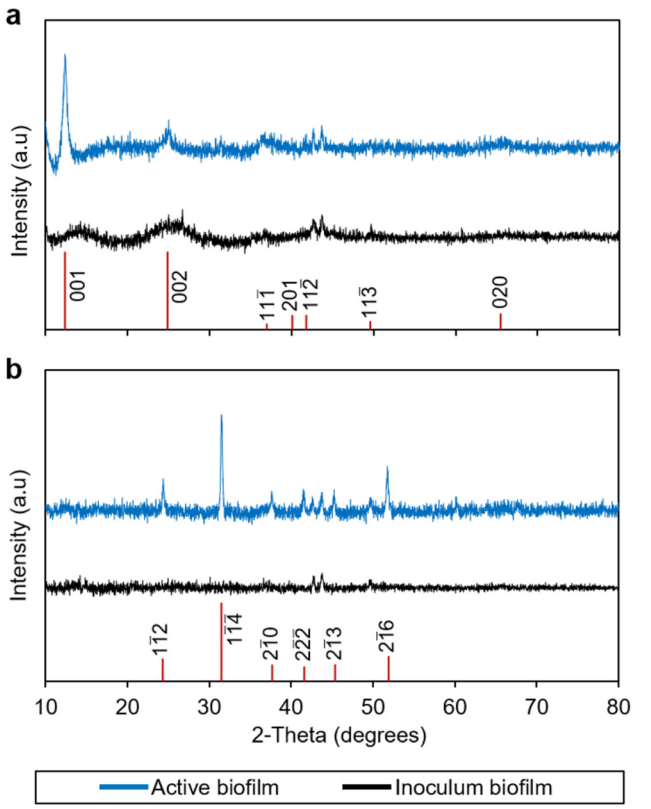

Fig. 3 – XRD patterns of the IB (in black) and the active biofilms (in blue) after the 42-day incubation for Sept (a) and Jan (b) experiments. The red lines indicate peak positions and Miller indices (*hkl*) defining reflections, adapted from the Crystallography Open Database (COD) for birnessite (in a) (COD 9013652 (ref. 56)) and rhodochrosite (in b) (COD 9007691 (ref. 67)). The XRD patterns from the Sept and Jan samples were relatively low in peak intensity and showed peak broadening, likely indicating either small crystal size, low crystallinity, amorphous structure, or the presence of impurities.

δ-MnO_2 is known as a promising and effective catalyst for removing ammonia,[63] organic water contaminants,[64] and oxidized metals;[65] therefore, its presence in BAC filters could be beneficial to perform a robust water treatment process to remove these types of contaminants. The XRD patterns of the active biofilms from the Jan experiments (Fig. 3b) showed that Mn was not fully oxidized and was still present as $MnCO_3$, as compared to XRD peaks of rhodochrosite (a pure $MnCO_3$ mineral) from the COD database (COD 9007691 (ref. 66)). This finding aligns with the ICP results, accounting for just half of the Mn^{2+} oxidized to insoluble forms (Table 2), and the SEM images showing the presence of residual $MnCO_3$ (Fig. 2e and f). In contrast to the high VSS values measured at the end of both experiments (Table 2), the lower yield of Mn oxidation in the Jan samples suggests that the microbial community which developed from these biofilms may have different Mn^{2+} conversion routes than the ones in the Sept samples. Nevertheless, similar nanoflower structures were observed in the Jan samples to those in the Sept ones (Fig. 2e and f). However, the exact type of MnOx forming these nanoflowers could not be distinguished in the Jan samples using XRD, likely due to the high concentration of untransformed $MnCO_3$ mixed with amorphous in proportion to the crystalline MnOx.

3.3 Microbial community enrichment into specialized MnOB populations

3.3.1 Selective enrichment of bacterial groups in all the replicates. In both Sept and Jan experiments, the phylum-level relative abundance of *Proteobacteria* relevantly increased when feeding Mn^{2+}, with a concurrent decrease in members of the phylum *Bacteroidota* that dominated the IB of both samplings (Fig. S5†). Within the phylum *Proteobacteria*, members of the orders *Rhizobiales* and *Burkholderiales* (formerly known as *Betaproteobacteriales*) had the highest increase after 42-day incubation (Fig. S5†). The majority of *Bacteroidota* in the IB whose relative abundance has decreased after 42 days were affiliated with the order *Chitinophagales* (Fig. S5†). Members of the two families of *Chitinophagales*, *Chitinophagaceae* and *Saprospiraceae*, were identified in biological filtration systems where nitrification, protein degradation, and removal of micropollutants were the prevailing metabolisms,[68,69] similar to the BAC filters from which the IB was sampled.[33] In the BAC filters, members of phylum *Nitrospirota* (mostly genus *Nitrospira*) were typically dominant,[33] but these decreased markedly in all the enrichment cultures (Fig. S5†), while Mn oxidizing activity remained. This despite the activity of MnOB in mixed cultures is often associated with the presence of active nitrifiers.[70]

Beta diversity analysis showed that the IB samples somewhat clustered, and thus had similar but not identical community compositions. Based on Bray–Curtis dissimilarities, this indicated comparable relative abundances of genera (Fig. 4). The marked change in the dominance of taxa in the enrichment described before caused a consistent shift in the community

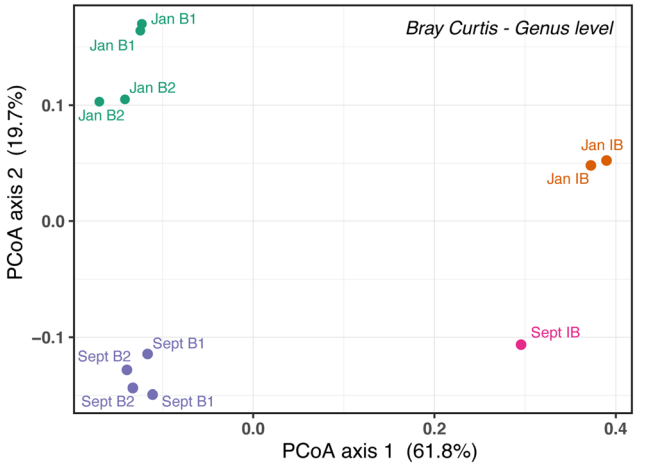

Fig. 4 – Beta diversity was analyzed as principal coordinates of Bray–Curtis dissimilarities among samples. Beta diversity shows clustering of inoculum communities (right) and active biofilms after 42 days (left) for Sept and Jan experiments in duplicate bottles (B1 and B2). Despite slight compositional differences between Sept (bottom half) and Jan (top half), the universal leftward shift indicates predictable changes in the relative abundances of the bacterial genera. Note that most variation in community composition is explained by PCoA axis 1.

composition for both Sept and Jan experiments (leftward in Fig. 4), even though differences among IB communities were partly maintained (*i.e.*, Sept and Jan remained segregated in the lower and upper part in Fig. 4, respectively).

This result was confirmed by analyzing the relative abundances of the dominant bacterial groups (>1%), where the same 14 bacterial groups increased significantly in both Sept and Jan experiments compared to their IBs (Fig. 5, green bar). This Mn-oxidizing community was mostly composed of members of the classes *Gammaproteobacteria* (20% to 25%) and *Alphaproteobacteria* (10% to 15%), and most of the dominant groups have been associated several times with Mn oxidation. Among these, *Pseudomonas* spp. are considered model microorganisms for Mn oxidation for which pathways and enzymes were partially characterized.[71–73] *Hydrogenophaga* species are associated with Mn oxidation in drinking water systems,[74] biofilters,[75] and other natural environments (*e.g.*, ref. 76).

Hyphomicrobium, belonging to the order *Rhizobiales*, was one of the first Mn oxidizers studied, responsible for the accumulation of MnOx in water pipelines[77] and biofilters.[75,78,79] Other Mn-oxidizing *Rhizobiales* were previously identified in various natural habitats,[9] and recent studies have discovered new species.[74,80] A well-known Mn-oxidizing *Rhizobiales* detected in the experimental bottles was *Pedomicrobium*[81] (Fig. 5), in which deposition of MnOx occurs in close association with EPS excretion,[82] as also observed in our cultures (Fig. 1f). Within *Rhizobiales*, members of the family *Xanthobacteraceae* were recently identified in Mn-rich rocks,[83] likely connected to their ability to survive in habitats with excessive accumulation of Mn.[84] The families A0839 and Amb-16S-1323 (Fig. 5) (just recently described and classified under *Rhizobiales* in the SILVA database release 138.1, and represented by uncultured strains) have not been associated with Mn-oxidizing ability before. All the

Affiliation	September IB	September B1	September B2	January IB	January B1	January B2
Comamonadaceae	3.9	9.8	13.1	2.4	10.1	9.4
Hyphomicrobium	1.9	3.9	4.4	1.0	4.4	5.8
Ellin6067	0.3	3.8	2.7	0.9	3.4	3.5
Hydrogenophaga	0.1	3.5	4.3	0.1	0.2	0.4
Pseudomonas	0.3	2.0	1.8	0.4	7.9	7.9
A0839	0.4	2.8	2.1	1.1	3.7	3.8
Pir4 lineage	1.3	2.6	2.2	1.3	2.6	2.9
Rhodococcus	0.2	2.4	3.8	0.1	1.4	1.9
Rhizobiales	0.3	1.4	1.2	0.1	0.9	0.7
Pirellulaceae	0.4	1.4	1.2	0.4	1.6	1.8
Amb-16S-1323	0.2	1.3	0.8	0.1	1.5	1.5
Gemmata	0.4	1.2	0.9	0.1	0.2	0.2
Xanthobacteraceae	0.3	0.6	0.6	0.2	2.1	2.2
SWB02	0.4	1.6	1.2	1.1	1.0	1.3
Candidatus Accumulibacter	0.0	1.1	0.7	0.1	0.1	0.1
Nevskia	0.1	0.1	0.1	0.0	3.7	0.8
Gemmataceae	2.3	2.2	1.8	1.0	1.5	1.6
Rhizobiales Incertae Sedis	0.9	0.9	1.0	0.4	1.0	1.0
Pedomicrobium	1.1	0.9	1.1	0.5	1.3	1.5
Rhizobiaceae	0.5	0.4	0.5	0.4	1.0	1.1
Vicinamibacterales	2.1	2.1	1.9	1.6	1.7	1.5
Planctomycetales	2.1	2.1	2.3	1.8	0.9	1.1
Oxalobacteraceae	1.1	1.5	1.2	0.9	0.1	0.1
Sphingorhabdus	0.3	0.3	0.3	1.1	0.3	0.2
Nitrospira	4.8	3.1	1.6	5.6	1.4	1.4
Terrimonas	4.9	2.3	2.9	10.5	8.9	4.3
Blastocatellaceae	5.2	2.2	3.3	3.6	2.4	2.3
Sphingomonadaceae	1.5	1.1	0.9	1.3	0.3	0.4
Reyranella	1.6	1.1	0.6	1.3	0.4	0.4
Rhodobacteraceae	0.9	0.6	0.8	0.5	1.2	1.2
Pirellula	0.9	0.5	0.6	1.2	0.6	0.7
Ferruginibacter	1.7	0.4	0.4	6.7	0.7	0.8
Saprospiraceae	7.7	0.3	0.3	2.5	0.2	0.2
Nitrosomonas	3.1	0.2	0.3	5.0	0.3	0.3
Sphingopyxis	2.3	0.2	0.4	0.9	0.6	0.6
Flavobacterium	4.4	0.1	0.1	4.5	0.1	0.1
Chitinophagaceae	1.3	0.1	0.1	2.2	0.2	0.1

Fig. 5 – Relative abundances (between 0% and 14%) of dominant bacterial ASVs (>1% relative abundance in at least one of the samples reported) comparing the inoculum biofilms (IBs) and active biofilms sampled at the end of Sept and Jan experiments in duplicate bottles (B1 and B2). Microbial groups were identified using 16S rRNA gene amplicon sequencing, and their taxonomy classification is reported at the identified level. Color bars on the right indicate the trend of each ASV in B1 and B2 in comparison with the IB: green (increasing), yellow (stable), and red (decreasing).

Rhizobiales not identified at the genus level, accounting for an average of 7% relative abundance in all the Mn-enriched communities, potentially correspond to undescribed Mn-oxidizing species. *Comamonadaceae*, formerly known as *Burkholderiaceae*, was a dominant family in all the active biofilm samples, with average relative abundances of 11.5% and 9.8% in the Sept and Jan experiments, respectively (Fig. 5). Recently, *Burkholderiaceae* were enriched in biofilms of BAC filters when loaded with nano-MnO_2 to optimize ammonium removal.[85] In metal-rich soils, *Burkholderiaceae* members play a key role by transforming different metals and by growing *via* chemolithoautotrophy.[86] Mn-oxidizing *Burkholderia* spp. were isolated from Mn nodules in rice field subsoils[87] and a Mn-rich soil layer.[88] *Burkholderia* spp. isolated from plants were also identified as Mn-solubilizing bacteria,[89] suggesting the same action on the $MnCO_3$ substrate in the enrichment cultures.

The other dominant groups have rarely been associated with Mn oxidation. Under the *Rhodococcus* genus, the species *R. opacus* was recently found to bioadsorb Mn^{2+}.[90] *Rhodococcus* was identified in the effluent of a biofilter performing Mn oxidation, but not on the filter media,[23] thus its association with Mn metabolism was not yet proven. Farda and colleagues[83] recently showed that *Rhodococcus* spp. was associated with Mn-solubilizing activity rather than its oxidation, an ability never reported before for this genus that may be fundamental for the cycling of this metal.

The putative ammonia-oxidizing *Ellin6067* is a genus of the family *Nitrosomonadaceae*, identified at relatively high abundance in both experiments (Fig. 5). *Ellin6067* is commonly found in soils[91] and detected in lab-scale experiments in the presence of a stress factor, such as high pharmaceutical concentrations,[92] light irradiation,[93] or the presence of cadmium.[94] *Ellin6067* is hypothesized to perform autotrophic denitrification under carbon limited conditions.[95] *Nitrosomonadaceae* in general were identified in nitrifying communities associated with MnOB in a lab-scale biofilm reactor,[70] in full-scale Mn-removing sand filters,[96] and in communities from Mn-rich rocks and associated water samples.[86] The substantial increase of *Ellin6067* from the IBs in the Sept and Jan experiments (Fig. 5) suggests a similar association with MnOB.

Potential association between *Planctomycetota* and Mn oxidation was recently demonstrated by Suarez and colleagues,[97] in biofilms sampled from marine deep subsurface.

Under this phylum, members of the family *Pirellulaceae* are commonly found in oligotrophic and extreme environments[98] and have been detected in Mn-rich environments and thus putatively associated with Mn oxidation.[99] The genus *Pir4* lineage was never associated with Mn oxidation, but one novel species under this genus was isolated from hydrothermal metalliferous deposits.[100]

Among the bacterial groups with a decreasing trend, *Terrimonas*, one of the dominant genera in both IBs (Fig. 5), persisted at averages of 2.6% and 6.6% relative abundances in the Sept and Jan experiments, respectively. They were reported to be able to oxidize Mn in natural environments such as rock varnish[101] and birnessite-type manganese deposits.[80]

3.3.2 Possible relationship between microbial communities and MnOx crystals. The observed dissimilarities in Mn oxidation behavior between the Sept and Jan experiments (Table 2, Fig. 3) could be related to the different abundances of certain microbial community members. For example, after the 42-day experiment, a relevant difference in the relative abundances between the Sept and Jan samples was observed for two key microbial groups, *Hydrogenophaga* and *Pseudomonas* (Fig. 5). *Hydrogenophaga* species, barely detected in the Jan bottles compared to the Sept ones, were associated with the formation of birnessite during anthracite-based biofiltration, which had a similar nanoflower structure as observed in this study (Fig. 3).[75] On the other hand, *Pseudomonas*, a dominant genus in the Jan bottles, had a 5-fold higher relative abundance in these samples than in the Sept ones, which could be related

to a leading role in the oxidation process and thus to the presence of an amorphous MnOx, as previously characterized from *Pseudomonas* pure cultures[71] and observed after XRD analysis (Fig. 3). In a study investigating the relationship between natural microorganisms and their ability to produce Mn oxides, X-ray absorption spectra and electron diffraction patterns showed that *Hydrogenophaga* was associated with polycrystalline birnessite, while *Nevskia*, an abundant genus in the Jan bottles (Fig. 5), was associated with MnOx with a lower oxidation state compared to the one formed by *Hydrogenophaga*, and a high amount of non-converted Mn^{2+} was adsorbed in its EPS.[102] Finally, a higher relative abundance of *Rhodococcus* in the Sept bottles (Fig. 5), recently hypothesized to be a Mn-solubilizing bacterium,[83] may have increased the release and availability of soluble Mn^{2+} from the $MnCO_3$ supplied as only a medium component, favoring in turn the cycle between soluble and insoluble Mn within the batch cultures.[9]

3.4 Importance of investigating Mn oxides from mixed microbial cultures in water treatment systems

Biogenic MnOx are frequently detected in water treatment systems such as biofilters, where black nodules form within the biofilm matrix growing on top of the filtration media.[14,15,22] These MnOx are of technological importance because they can be used to improve water treatment performances and environmental remediation. Biogenic MnOx indeed can adsorb and oxidize toxic metals (*e.g.*, lead, chromium, arsenic, and cadmium) and organic matter,[11] boosting the degradation of a wide array of compounds, including recalcitrant pollutants, through various mechanisms.[7] Interestingly, the concentration of some selected micropollutants in the IB samples, originating from the full-scale BAC filter, substantially decreased from day 0 to day 42 in the Sept experiment, when biofilms developed and were enriched with biogenic δ-MnO_2 (Fig. S6†). This decrease could be due to either adsorption or oxidation mechanisms involving the crystalline structure of the oxides. A better understanding of the properties of MnOx formed by biofilm mixed microbial cultures in such filtration systems is thus of interest, particularly to determine if they improve the water treatment performances. MnOB communities within water filtration systems could be seen as a cost-effective method to efficiently produce high-quality catalysts. In this study, we have shown that mixed microbial communities in biofilms sampled from an oxygen-augmented BAC filtration system efficiently convert Mn^{2+} into MnOx under oligotrophic conditions, growing a consistent floccular EPS-rich biofilm (Fig. 1, Table 1) that encompasses black nodules of birnessite-type minerals (Fig. 1 and 3), organized in nanoflower structures with nano-layered crystals (Fig. 2). The EPS matrix of biofilms plays a fundamental role in Mn adsorption and oxidation,[103,104] as Mn-oxidizing organisms utilize secreted organic molecules as templates for mineral growth.[105] There is a strong connection between biomacromolecules and MnOx deposition in natural environments;[106] this connects with the role of MnOx not only in converting, but likely also in preserving organic carbon under oligotrophic conditions.[107] The microbial enzymatic oxidation activity contributes to the continuous regeneration of MnOx nodules within the biofilm, making their catalytic properties potentially unlimited as long as Mn^{2+} is present in the medium.[108] As the reactivity of MnOx with metal cations depends on the fine structure of the oxides,[8] the presence of MnOB should be coupled with the formation of highly crystalline oxides (having a high surface area) with a high oxidation state.[64] Therefore, detailed knowledge of MnOx structures formed by microorganisms living under a variety of environmental conditions can provide insight into how they can ultimately be applied as catalysts. Most of the knowledge on the catalytic potential of biogenic MnOx comes from the model microorganisms *Bacillus* sp. strain SG-1, *Pseudomonas putida* strain MnB1, and *Leptothrix discophora* strain SS-1.[8,104,109] These bacteria form layered birnessite with a poor crystalline structure[8] as often observed for other biogenic MnOx characterized to date at a lab-scale.[110] Several studies have utilized pure culture bacteria grown in a rich culture medium to produce MnOx, testing their efficiency towards adsorption/oxidation of metals, dye decolorization and degradation of organic contaminants at a lab-scale (*i.e.*, ref. 108, 111, and 112).

In contrast, in this work we used mixed microbial communities that were not provided with any macronutrients besides the ones already present in the inoculum water (Table S1†). The addition of $MnCO_3$ as a source of Mn^{2+} ensured a slow release of the substrate, mimicking Mn cycling as it happens in natural environments.[13] Under these oligotrophic conditions, XRD profiles showed the formation of birnessite (or δ-MnO_2) (Fig. 3b) with a nanoflower morphology (Fig. 2), similar to the chemically synthesized δ-MnO_2,[48,59] applied as a catalyst for the decomposition of recalcitrant compounds.[113] The 3D nanoflower morphology ensures a high surface to volume ratio, enhancing surface adsorption and charge transfer, and accelerating the kinetics of reactions.[114] The redox and adsorption properties of biogenic MnOx may provide increased access to both biodegradable and recalcitrant materials for biodegradation, thus being beneficial for water treatment in general. By means of 16S rRNA gene sequencing, we identified several bacterial groups in the enrichment cultures (Fig. 5) likely connected to either the solubilization or the oxidation of Mn. By studying the microbial community in full-scale biofilters connected to wastewater reuse, this study implements the knowledge in the biofiltration field which is often limited to the treatment of surface and ground water to produce drinking water. To date, the characterized biochemical mechanisms associated with Mn oxidation are confined to a few isolated strains, thus the list of Mn oxidation enzymes is still very limited.[9] Overall, future work should focus on further structural characterization of MnOx formed by mixed microbial cultures and linking it to their catalytic potential, and on defining the enzymology of more microbial species for this almost ubiquitous, yet poorly understood microbial function.

4 Conclusions

- The detached biofilms from aged, oxygen augmented BAC granules from a wastewater reclamation plant harbor a diverse microbial community that shows chemolithoautotrophic growth as a result of Mn^{2+} oxidation.

- Specific enrichment for MnOB from BAC biofilms using $MnCO_3$, due to its low solubility in water, ensures the continuous presence of soluble Mn^{2+}, mimicking the conditions of a full-scale BAC filter where Mn is continuously present in the influent at low concentrations.

- Opposite to pure cultures of model microorganisms, enriched oligotrophic mixed microbial communities with a variety of MnOB groups result in the formation of nanoflower crystals of birnessite (δ-MnO_2).

- Biotechnological contexts, where MnOB originating from natural environments find a suitable habitat to adhere and grow in mixed microbial communities, are potential sources of biological MnOx catalysts.

- The understanding of biogenic MnOx formation by mixed microbial cultures, naturally present in biofilters, may be advantageous to stimulate this ability *in situ* and thus to optimize performances towards the removal of recalcitrant organics and metals from water.

Data availability

16S rRNA gene sequencing data used for microbial community analysis were deposited in the European Nucleotide Archive (ENA) (**https://www.ebi.ac.uk/ena/browser/home**), under the project number PRJEB64232. The other data supporting this article have been included as part of the manuscript and the ESI.†

Conflicts of interest

There are no conflicts to declare.

Acknowledgements

This work was supported by the cooperation framework of Wetsus, European Centre of Excellence for Sustainable Water Technology (**https://www.wetsus.eu**). Wetsus is co-funded by the Dutch Ministry of Economic Affairs and Ministry of Infrastructure and Environment, the European Union Regional Development Fund, the Province of Fryslan and the Northern Netherlands Provinces. The authors thank the Wetsus analytical team, especially Jelmer Dijkstra for his valuable help with the manganese speciation measurement and Agnieszka Tomaszewska for conducting SEM imaging. We acknowledge Prof. Jared R. Leadbetter (California Institute of Technology, US) for his valuable advice to prepare the Mn-enrichment experiments, Kaylee Bol for the laboratory work with the DNA extraction, and Ing. Jacob Baas (Zernike Institute for Advanced Materials, NL) for operating the XRD analysis. We also thank Nieuwater, the members of Advanced Water Treatment Theme, and the Foundation for Applied Water Research in The Netherlands (STOWA) for the shared knowledge and financial support.

References

1 J. E. Post, Manganese Oxide Minerals: Crystal Structures and Economic and Environmental Significance, *Proc. Natl. Acad. Sci. U. S. A.*, 1999, **96**, 3447–3454.
2 A. Postawa, C. Hayes, A. Criscuoli, F. Macedonio, A. N. Angelakis, J. B. Rose, A. Maier and D. C. McAvoy, *Best Practice Guide on the Control of Iron and Manganese in Water Supply*, IWA Publishing, 2013.
3 K. H. Nealson, in *The Prokaryotes*, ed. M. Dworkin, S. Falkow, E. Rosenberg, K.-H. Schleifer and E. Stackebrandt, Springer New York, New York, NY, 2006, pp. 222–231.
4 J. J. Morgan, Kinetics of reaction between O2 and Mn(II) species in aqueous solutions, *Geochim. Cosmochim. Acta*, 2005, **69**, 35–48.
5 J. L. Junta and M. F. Hochella, Manganese (II) oxidation at mineral surfaces: A microscopic and spectroscopic study, *Geochim. Cosmochim. Acta*, 1994, **58**, 4985–4999.
6 B. M. Tebo, B. G. Clement and G. J. Dick, in *Manual of Environmental Microbiology*, John Wiley & Sons, Ltd, 2007, pp. 1223–1238.
7 B. M. Tebo, J. R. Bargar, B. G. Clement, G. J. Dick, K. J. Murray, D. Parker, R. Verity and S. M. Webb, Biogenic Manganese Oxides: Properties and Mechanisms of Formation, *Annu. Rev. Earth Planet. Sci.*, 2004, **32**, 287–328.
8 T. G. Spiro, J. R. Bargar, G. Sposito and B. M. Tebo, Bacteriogenic Manganese Oxides, *Acc. Chem. Res.*, 2010, **43**, 2–9.
9 B. M. Tebo, H. A. Johnson, J. K. McCarthy and A. S. Templeton, Geomicrobiology of manganese(II) oxidation, *Trends Microbiol.*, 2005, **13**, 421–428.
10 L. Jia, Q. Zhou, Y. Li and W. Wu, Application of manganese oxides in wastewater treatment: Biogeochemical Mn cycling driven by bacteria, *Chemosphere*, 2023, **336**, 139219.
11 H. Zhou and C. Fu, Manganese-oxidizing microbes and biogenic manganese oxides: characterization, Mn(II) oxidation mechanism and environmental relevance, *Rev. Environ. Sci. Biotechnol.*, 2020, **19**, 489–507.
12 P. P. Sujith and P. A. L. Bharathi, in *Molecular Biomineralization: Aquatic Organisms Forming Extraordinary Materials*, ed. W. E. G. Müller, Springer, Berlin, Heidelberg, 2011, pp. 49–76.
13 H. Yu and J. R. Leadbetter, Bacterial chemolithoautotrophy via manganese oxidation, *Nature*, 2020, **583**, 453–458.
14 D. R. Bernstein, G. D. E. Glasgow, M. C. Lay and M. Manley-Harris, Accumulation of manganese oxides in biological activated carbon filters: Implications for biodegradation studies, *AWWA Water Sci.*, 2022, **4**, e1300.
15 W. Hu, J. Liang, F. Ju, Q. Wang, R. Liu, Y. Bai, H. Liu and J. Qu, Metagenomics Unravels Differential Microbiome Composition and Metabolic Potential in Rapid Sand Filters Purifying Surface Water Versus Groundwater, *Environ. Sci. Technol.*, 2020, **54**, 5197–5206.

16 G. Li, X. Ma, R. Chen, Y. Yu, H. Tao and B. Shi, Field studies of manganese deposition and release in drinking water distribution systems: Insight into deposit control, *Water Res.*, 2019, **163**, 114897.
17 J. E. Tobiason, A. Bazilio, J. Goodwill, X. Mai and C. Nguyen, Manganese Removal from Drinking Water Sources, *Curr. Pollut. Rep.*, 2016, **2**, 168–177.
18 L. Ciancio Casalini, A. Piazza, F. Masotti, V. A. Pacini, G. Sanguinetti, J. Ottado and N. Gottig, Manganese removal efficiencies and bacterial community profiles in non-bioaugmented and in bioaugmented sand filters exposed to different temperatures, *J. Water Process Eng.*, 2020, **36**, 101261.
19 D. M. Sahabi, M. Takeda, I. Suzuki and J. Koizumi, Removal of Mn2+ from water by "aged" biofilter media: The role of catalytic oxides layers, *J. Biosci. Bioeng.*, 2009, **107**, 151–157.
20 W.-W. Li and H.-Q. Yu, Insight into the roles of microbial extracellular polymer substances in metal biosorption, *Bioresour. Technol.*, 2014, **160**, 15–23.
21 J. Tourney and B. T. Ngwenya, The role of bacterial extracellular polymeric substances in geomicrobiology, *Chem. Geol.*, 2014, **386**, 115–132.
22 N. E. McCormick, M. Earle, C. Ha, L. Hakes, A. Evans, L. Anderson, A. K. Stoddart, M. G. I. Langille and G. A. Gagnon, Biological and physico-chemical mechanisms accelerating the acclimation of Mn-removing biofilters, *Water Res.*, 2021, **207**, 117793.
23 N. E. McCormick, M. Earle, A. K. Stoddart, M. G. I. Langille and G. A. Gagnon, Understanding the impact of different source water types on the biofilm characteristics and microbial communities of manganese removing biofilters, *Environ. Sci.: Water Res. Technol.*, 2023, **9**, 48–61.
24 J. A. Charbonnet, Y. Duan and D. L. Sedlak, The use of manganese oxide-coated sand for the removal of trace metal ions from stormwater, *Environ. Sci.: Water Res. Technol.*, 2020, **6**, 593–603.
25 K. Lin, Y. Peng, X. Huang and J. Ding, Transformation of bisphenol A by manganese oxide-coated sand, *Environ. Sci. Pollut. Res.*, 2013, **20**, 1461–1467.
26 M. J. Kirisits, M. B. Emelko and A. J. Pinto, Applying biotechnology for drinking water biofiltration: advancing science and practice, *Curr. Opin. Biotechnol.*, 2019, **57**, 197–204.
27 Z. Lu, W. Sun, C. Li, W. Cao, Z. Jing, S. Li, X. Ao, C. Chen and S. Liu, Effect of granular activated carbon pore-size distribution on biological activated carbon filter performance, *Water Res.*, 2020, **177**, 115768.
28 Z. Lu, Z. Jing, J. Huang, Y. Ke, C. Li, Z. Zhao, X. Ao and W. Sun, Can we shape microbial communities to enhance biological activated carbon filter performance?, *Water Res.*, 2022, **212**, 118104.
29 W. Qi, W. Li, J. Zhang, X. Wu, J. Zhang and W. Zhang, Effect of biological activated carbon filter depth and backwashing process on transformation of biofilm community, *Front. Environ. Sci. Eng.*, 2019, **13**, 15.
30 A. E. Keithley, H. Ryu, V. Gomez-Alvarez, S. Harmon, C. Bennett-Stamper, D. Williams and D. A. Lytle, Comprehensive characterization of aerobic groundwater biotreatment media, *Water Res.*, 2023, **230**, 119587.
31 W. R. Morales Medina, P. To, M. Taylor, C. Nguyen and N. L. Fahrenfeld, Acclimation, manganese removal, and backwash impact on full-scale drinking water biofilter microbiome, *AWWA Water Sci.*, 2023, **5**, e1334.
32 P. van der Maas, G. Veenendaal, J. Nonnekens, H. Brink and D. de Vogel, Biologische actiefkoolfiltratie met zuurstofdosering: veelbelovende techniek voor verwijdering geneesmiddelen?, *H2O/Waternetwerk (online)*, 2020, **https://www.h2owaternetwerk.nl/vakartikelen/biologische-actiefkoolfiltratie-met-zuurstofdosering-veelbelovende-techniek-voor-verwijdering-geneesmiddelen**.
33 O. Bernadet, A. Larasati, H. P. J. Van Veelen, G. J. W. Euverink and M. C. Gagliano, Biological Oxygen-dosed Activated Carbon (BODAC) filters – A bioprocess for ultrapure water production removing organics, nutrients and micropollutants, *J. Hazard. Mater.*, 2023, **458**, 131882.
34 S. Ribeiro Pinela, A. Larasati, R. J. W. Meulepas, M. C. Gagliano, R. Kleerebezem, H. Bruning and H. H. M. Rijnaarts, Ultrafiltration (UF) and biological oxygen-dosed activated carbon (BODAC) filtration to prevent fouling of reversed osmosis (RO) membranes: A mass balance analysis, *J. Water Process Eng.*, 2024, **57**, 104648.
35 I. Saratovsky, P. G. Wightman, P. A. Pastén, J.-F. Gaillard and K. R. Poeppelmeier, Manganese Oxides: Parallels between Abiotic and Biotic Structures, *J. Am. Chem. Soc.*, 2006, **128**, 11188–11198.
36 S. Namgung and G. Lee, Rhodochrosite Oxidation by Dissolved Oxygen and the Formation of Mn Oxide Product: The Impact of Goethite as a Foreign Solid Substrate, *Environ. Sci. Technol.*, 2021, **55**, 14436–14444.
37 Y. Tang, C. A. Zeiner, C. M. Santelli and C. M. Hansel, Fungal oxidative dissolution of the Mn(II)-bearing mineral rhodochrosite and the role of metabolites in manganese oxide formation, *Environ. Microbiol.*, 2013, **15**, 1063–1077.
38 H. Wang and X. Pan, Role of extracellular polymeric substances (EPS) from Pseudomonas putida strain MnB1 in dissolution of natural rhodochrosite, *Biogeosci. Discuss.*, 2014, **11**, 7273–7290.
39 EPA, *Standard Methods for the Examination of Water and Wastewater*, 14th edn, 1975, p. 95, Method 208E.
40 G. A. O'Toole, L. A. Pratt, P. I. Watnick, D. K. Newman, V. B. Weaver and R. Kolter, Genetic approaches to study of biofilms, *Methods Enzymol.*, 1999, **310**, 91–109.
41 H. Yu and J. R. Leadbetter, Bacterial chemolithoautotrophy via manganese oxidation, *Nature*, 2020, **583**, 453–458.
42 A. E. Parada, D. M. Needham and J. A. Fuhrman, Every base matters: assessing small subunit rRNA primers for marine microbiomes with mock communities, time series and global field samples, *Environ. Microbiol.*, 2016, **18**, 1403–1414.
43 C. Quince, A. Lanzen, R. J. Davenport and P. J. Turnbaugh, Removing Noise From Pyrosequenced Amplicons, *BMC Bioinf.*, 2011, **12**, 38.

44 E. Bolyen, *et al.*, Reproducible, interactive, scalable and extensible microbiome data science using QIIME 2, *Nat. Biotechnol.*, 2019, **37**, 852–857.
45 B. J. Callahan, P. J. McMurdie, M. J. Rosen, A. W. Han, A. J. A. Johnson and S. P. Holmes, DADA2: High-resolution sample inference from Illumina amplicon data, *Nat. Methods*, 2016, **13**, 581–583.
46 C. Quast, E. Pruesse, P. Yilmaz, J. Gerken, T. Schweer, P. Yarza, J. Peplies and F. O. Glöckner, The SILVA ribosomal RNA gene database project: improved data processing and web-based tools, *Nucleic Acids Res.*, 2013, **41**, 590–596.
47 S. Furuta, H. Ikegaya, M. Fujibayashi, H. Hashimoto, S. Suzuki, K. Okano, S. Ichise and N. Miyata, Effects of Algal Extracellular Polymeric Substances on the Formation of Filamentous Manganese Oxide Particles in the near-Bottom Layer of Lake Biwa, *Microorganisms*, 2023, **11**(7), 1814.
48 Y. Li, G. Jiang, N. Ouyang, Z. Qin, S. Lan and Q. Zhang, The Controlled Synthesis of Birnessite Nanoflowers via H2O2 Reducing KMnO4 For Efficient Adsorption and Photooxidation Activity, *Front. Chem.*, 2021, **9**, 699513.
49 Y.-H. Lin and B.-H. Ho, Kinetics and Performance of Biological Activated Carbon Reactor for Advanced Treatment of Textile Dye Wastewater, *Processes*, 2022, **10**, 129.
50 L. Piai, J. Dykstra, A. van der Wal and A. Langenhoff, Bioaugmentation of Biological Activated Carbon Filters for Enhanced Micropollutant Removal, *ACS ES&T Water*, 2022, **2**, 2359–2366.
51 E. J. Arcuri and H. L. Ehrlich, in *Biogeochemistry of Ancient and Modern Environments*, ed. P. A. Trudinger, M. R. Walter and B. J. Ralph, Springer, Berlin, Heidelberg, 1980, pp. 339–344.
52 H. L. Ehrlich and J. C. Salerno, Energy coupling in Mn2+ oxidation by a marine bacterium, *Arch. Microbiol.*, 1990, **154**, 12–17.
53 H. L. Ehrlich, Inorganic energy sources for chemolithotrophic and mixotrophic bacteria, *Geomicrobiol. J.*, 1978, **1**, 65–83.
54 D. E. LaRowe, H. K. Carlson and J. P. Amend, The Energetic Potential for Undiscovered Manganese Metabolisms in Nature, *Front. Microbiol.*, 2021, **12**, 636145.
55 E. J. Elzinga, Reductive Transformation of Birnessite by Aqueous Mn(II), *Environ. Sci. Technol.*, 2011, **45**, 6366–6372.
56 C. L. Lopano, P. J. Heaney and J. E. Post, Cs-exchange in birnessite: Reaction mechanisms inferred from time-resolved X-ray diffraction and transmission electron microscopy, *Am. Mineral.*, 2009, **94**, 816–826.
57 C. F. Holder and R. E. Schaak, Tutorial on Powder X-ray Diffraction for Characterizing Nanoscale Materials, *ACS Nano*, 2019, **13**, 7359–7365.
58 D. M. Robinson, Y. B. Go, M. Mui, G. Gardner, Z. Zhang, D. Mastrogiovanni, E. Garfunkel, J. Li, M. Greenblatt and G. C. Dismukes, Photochemical Water Oxidation by Crystalline Polymorphs of Manganese Oxides: Structural Requirements for Catalysis, *J. Am. Chem. Soc.*, 2013, **135**, 3494–3501.
59 X. Liang, Z. Zhao, M. Zhu, F. Liu, L. Wang, H. Yin, G. Qiu, F. Cao, X. Liu and X. Feng, Self-assembly of birnessite nanoflowers by staged three-dimensional oriented attachment, *Environ. Sci.: Nano*, 2017, **4**, 1656–1669.
60 M. Qin, H. Zhao, W. Yang, Y. Zhou and F. Li, A facile one-pot synthesis of three-dimensional microflower birnessite (δ-MnO2) and its efficient oxidative degradation of rhodamine B, *RSC Adv.*, 2016, **6**, 23905–23912.
61 J. Wang, J. Zhu, X. Zhou, Y. Du, W. Huang, J. Liu, W. Zhang, J. Shi and H. Chen, Nanoflower-like weak crystallization manganese oxide for efficient removal of low-concentration NO at room temperature, *J. Mater. Chem. A*, 2015, **3**, 7631–7638.
62 J. Hou, Y. Xiang, D. Zheng, Y. Li, S. Xue, C. Wu, W. Hartley and W. Tan, Morphology-dependent enhancement of arsenite oxidation to arsenate on birnessite-type manganese oxide, *Chem. Eng. J.*, 2017, **327**, 235–243.
63 C. Cheng, Q. He, J. Zhang, H. Chai, Y. Yang, S. G. Pavlostathis and H. Wu, New insight into ammonium oxidation processes and mechanisms mediated by manganese oxide in constructed wetlands, *Water Res.*, 2022, **215**, 118251.
64 C. K. Remucal and M. Ginder-Vogel, A critical review of the reactivity of manganese oxides with organic contaminants, *Environ. Sci.: Processes Impacts*, 2014, **16**, 1247–1266.
65 M. Li, S. Kuang, Y. Kang, H. Ma, J. Dong and Z. Guo, Recent advances in application of iron-manganese oxide nanomaterials for removal of heavy metals in the aquatic environment, *Sci. Total Environ.*, 2022, **819**, 153157.
66 E. N. Maslen, V. A. Streltsov, N. R. Streltsova and N. Ishizawa, Electron density and optical anisotropy in rhombohedral carbonates. III. Synchrotron X-ray studies of $CaCO_3$, $MgCO_3$ and $MnCO_3$, *Acta Crystallogr., Sect. B: Struct. Sci.*, 1995, **51**, 929–939.
67 E. N. Maslen, V. A. Streltsov, N. R. Streltsova and N. Ishizawa, Electron density and optical anisotropy in rhombohedral carbonates. III. Synchrotron X-ray studies of CaCO3, MgCO3 and MnCO3, *Acta Crystallogr., Sect. B: Struct. Sci.*, 1995, **51**, 929–939.
68 R. P. Bartelme, S. L. McLellan and R. J. Newton, Freshwater Recirculating Aquaculture System Operations Drive Biofilter Bacterial Community Shifts around a Stable Nitrifying Consortium of Ammonia-Oxidizing Archaea and Comammox Nitrospira, *Front. Microbiol.*, 2017, **8**, 101.
69 E. Ouyang, Y. Liu, J. Ouyang and X. Wang, Effects of different wastewater characteristics and treatment techniques on the bacterial community structure in three pharmaceutical wastewater treatment systems, *Environ. Technol.*, 2019, **40**, 329–341.
70 L. T. T. Cao, H. Kodera, K. Abe, H. Imachi, Y. Aoi, T. Kindaichi, N. Ozaki and A. Ohashi, Biological oxidation of Mn(II) coupled with nitrification for removal and recovery of minor metals by downflow hanging sponge reactor, *Water Res.*, 2015, **68**, 545–553.
71 S. Cömert and O. Tepe, Production and Characterization of Biogenic Manganese Oxides by Manganese-adapted Pseudomonas putida NRRL B-14878, *Geomicrobiol. J.*, 2020, **37**, 753–763.
72 K. Geszvain, J. K. McCarthy and B. M. Tebo, Elimination of Manganese(II,III) Oxidation in Pseudomonas putida GB-1

by a Double Knockout of Two Putative Multicopper Oxidase Genes, *Appl. Environ. Microbiol.*, 2013, **79**, 357–366.

73 M. Okazaki, T. Sugita, M. Shimizu, Y. Ohode, K. Iwamoto, E. W. de Vrind-de Jong, J. P. de Vrind and P. L. Corstjens, Partial purification and characterization of manganese-oxidizing factors of Pseudomonas fluorescens GB-1, *Appl. Environ. Microbiol.*, 1997, **63**, 4793–4799.

74 D. N. Marcus, A. Pinto, K. Anantharaman, S. A. Ruberg, E. L. Kramer, L. Raskin and G. J. Dick, Diverse manganese(II)-oxidizing bacteria are prevalent in drinking water systems, *Environ. Microbiol. Rep.*, 2017, **9**, 120–128.

75 S. Dangeti, J. M. McBeth, B. Roshani, J. M. Vyskocil, B. Rindall and W. Chang, Microbial communities and biogenic Mn-oxides in an on-site biofiltration system for cold Fe-(II)- and Mn(II)-rich groundwater treatment, *Sci. Total Environ.*, 2020, **710**, 136386.

76 S. Sjöberg, C. W. Stairs, B. Allard, F. Homa, T. Martin, V. Sjöberg, T. J. G. G. Ettema and C. Dupraz, Microbiomes in a manganese oxide producing ecosystem in the Ytterby mine, Sweden: Impact on metal mobility, *FEMS Microbiol. Ecol.*, 2020, **96**, 1–17.

77 P. A. Tyler and K. C. Marshall, Form and function in manganese-oxidizing bacteria, *Arch. Microbiol.*, 1967, **56**, 344–353.

78 X. Zhao, B. Liu, X. Wang, C. Chen, N. Ren and D. Xing, Single molecule sequencing reveals response of manganese-oxidizing microbiome to different biofilter media in drinking water systems, *Water Res.*, 2020, **171**, 115424.

79 J. Zheng, D. Li, H. Zeng, S. Yang, Z. Zhang and J. Zhang, Effect of Fe(II) on manganese removal in biofilters: Microbial community, formation of manganese oxide and related mechanisms, *J. Water Process Eng.*, 2023, **56**, 104519.

80 S. Sjöberg, C. W. Stairs, B. Allard, F. Homa, T. Martin, V. Sjöberg, T. J. G. Ettema and C. Dupraz, Microbiomes in a manganese oxide producing ecosystem in the Ytterby mine, Sweden: impact on metal mobility, *FEMS Microbiol. Ecol.*, 2020, **96**, fiaa169.

81 E. I. Larsen, L. I. Sly and A. G. McEwan, Manganese(II) adsorption and oxidation by whole cells and a membrane fraction of Pedomicrobium sp. ACM 3067, *Arch. Microbiol.*, 1999, **171**, 257–264.

82 L. I. Sly, V. Arunpairojana and D. R. Dixon, Binding of Colloidal MnO2 by Extracellular Polysaccharides of Pedomicrobium manganicum, *Appl. Environ. Microbiol.*, 1990, **56**, 2791–2794.

83 B. Farda, R. Djebaili, M. Del Gallo, C. Ercole, F. Bellatreccia and M. Pellegrini, The "Infernaccio" Gorges: Microbial Diversity of Black Deposits and Isolation of Manganese-Solubilizing Bacteria, *Biology*, 2022, **11**, 1204.

84 C. Li, C. Liu, C. Feng and T. Lan, Exploring the impacts of service life of biological activated carbon on dissolved organic nitrogen removal, *Environ. Pollut.*, 2023, **323**, 121214.

85 W. Qin, Q. Xiao, M. Hong, J. Yang, Y. Song and J. Ma, Nano manganese dioxide coupling carbon source preloading granular activated carbon biofilter enhancing biofilm formation and pollutant removal, *Environ. Res.*, 2024, **241**, 117606.

86 L. Li, D. Meng, H. Yin, T. Zhang and Y. Liu, Genome-resolved metagenomics provides insights into the ecological roles of the keystone taxa in heavy-metal-contaminated soils, *Front. Microbiol.*, 2023, **14**, 1203164.

87 V. R. Cahyani, J. Murase, E. Ishibashi, S. Asakawa and M. Kimura, Phylogenetic positions of Mn2+–oxidizing bacteria and fungi isolated from Mn nodules in rice field subsoils, *Biol. Fertil. Soils*, 2009, **45**, 337–346.

88 D. M. Akob, T. Bohu, A. Beyer, F. Schäffner, M. Händel, C. A. Johnson, D. Merten, G. Büchel, K. U. Totsche and K. Küsel, Identification of Mn(II)-Oxidizing Bacteria from a Low-pH Contaminated Former Uranium Mine, *Appl. Environ. Microbiol.*, 2014, **80**, 5086–5097.

89 C. F. Tullii, C. R. Alexandrino, N. D. da Silva, F. L. Olivares, U. Zottich, V. M. Gomes and M. Da Cunha, Identifying bioactive compounds and beneficial microorganisms associated with colleters in Palicourea tetraphylla (Rubiaceae), *S. Afr. J. Bot.*, 2023, **160**, 328–337.

90 A. M. R. Pimentel, P. R. Quispe, R. J. C. Torres, L. G. V. Gonzales, C. A. C. Olivera, A. G. Merma, I. D. dos Santos and M. L. Torem, Kinetic study and thermodynamic equilibrium modeling of the Co(II) and Mn(II) bioadsorption using the *Rhodococcus opacus* strain, *REM - International Engineering Journal*, 2022, **75**, 137–146.

91 J. Ye, R. Zhang, S. Nielsen, S. D. Joseph, D. Huang and T. Thomas, A Combination of Biochar–Mineral Complexes and Compost Improves Soil Bacterial Processes, Soil Quality, and Plant Properties, *Front. Microbiol.*, 2016, **7**, 372.

92 M. A. P. Vega, R. C. Scholes, A. R. Brady, R. A. Daly, A. B. Narrowe, L. B. Bosworth, K. C. Wrighton, D. L. Sedlak and J. O. Sharp, Pharmaceutical Biotransformation is Influenced by Photosynthesis and Microbial Nitrogen Cycling in a Benthic Wetland Biomat, *Environ. Sci. Technol.*, 2022, **56**, 14462–14477.

93 L. Wang, S. Qiu, J. Guo and S. Ge, Light Irradiation Enables Rapid Start-Up of Nitritation through Suppressing nxrB Gene Expression and Stimulating Ammonia-Oxidizing Bacteria, *Environ. Sci. Technol.*, 2021, **55**, 13297–13305.

94 J. Qu, Y. Yuan, X. Zhang, L. Wang, Y. Tao, Z. Jiang, H. Yu, M. Dong and Y. Zhang, Stabilization of lead and cadmium in soil by sulfur-iron functionalized biochar: Performance, mechanisms and microbial community evolution, *J. Hazard. Mater.*, 2022, **425**, 127876.

95 Y. Chen, Z. Shao, Z. Kong, L. Gu, J. Fang and H. Chai, Study of pyrite based autotrophic denitrification system for low-carbon source stormwater treatment, *J. Water Process Eng.*, 2020, **37**, 101414.

96 K. S. Nitzsche, P. Weigold, T. Lösekann-Behrens, A. Kappler and S. Behrens, Microbial community composition of a household sand filter used for arsenic, iron, and manganese removal from groundwater in Vietnam, *Chemosphere*, 2015, **138**, 47–59.

97 S. Suarez, J. M. Lema and F. Omil, Removal of Pharmaceutical and Personal Care Products (PPCPs) under

nitrifying and denitrifying conditions, *Water Res.*, 2010, **44**, 3214–3224.

98 H. Schlesner, C. Rensmann, B. J. Tindall, D. Gade, R. Rabus, S. Pfeiffer and P. Hirsch, Taxonomic heterogeneity within the Planctomycetales as derived by DNA-DNA hybridization, description of Rhodopirellula baltica gen. nov., sp. nov., transfer of Pirellula marina to the genus Blastopirellula gen. nov. as Blastopirellula marina comb. nov. and emended description of the genus Pirellula, *Int. J. Syst. Evol. Microbiol.*, 2004, **54**, 1567–1580.

99 M. Colombo, J. LaRoche, D. Desai, J. Li and M. T. Maldonado, Control of particulate manganese (Mn) cycling in halocline Arctic Ocean waters by putative Mn-oxidizing bacterial dynamics, *Limnol. Oceanogr.*, 2023, **68**, 2070–2087.

100 J. E. Storesund, A. Lanzèn, A. García-Moyano, A.-L. Reysenbach and L. Øvreås, Diversity patterns and isolation of Planctomycetes associated with metalliferous deposits from hydrothermal vent fields along the Valu Fa Ridge (SW Pacific), *Antonie van Leeuwenhoek*, 2018, **111**, 841–858.

101 S. K. Carmichael and S. L. Bräuer, in *Microbial Life of Cave Systems*, ed. A. Summers Engel, DE GRUYTER, 2015, pp. 137–160.

102 S. Sjöberg, C. Yu, C. W. Stairs, B. Allard, R. Hallberg, S. Henriksson, M. Åström and C. Dupraz, Microbe-Mediated Mn Oxidation—A Proposed Model of Mineral Formation, *Minerals*, 2021, **11**, 1146.

103 C. Li, S. Wang, X. Du, X. Cheng, M. Fu, N. Hou and D. Li, Immobilization of iron- and manganese-oxidizing bacteria with a biofilm-forming bacterium for the effective removal of iron and manganese from groundwater, *Bioresour. Technol.*, 2016, **220**, 76–84.

104 B. Toner, S. Fakra, M. Villalobos, T. Warwick and G. Sposito, Spatially Resolved Characterization of Biogenic Manganese Oxide Production within a Bacterial Biofilm, *Appl. Environ. Microbiol.*, 2005, **71**, 1300–1310.

105 D. Emerson, R. E. Garen and W. C. Ghiorse, Formation of Metallogenium-like structures by a manganese-oxiding fungus, *Arch. Microbiol.*, 1989, **151**, 223–231.

106 X. Huangfu, C. Ma, R. Huang, Q. He, C. Liu, J. Zhou, J. Jiang, J. Ma, Y. Zhu and M. Huang, Deposition Kinetics of Colloidal Manganese Dioxide onto Representative Surfaces in Aquatic Environments: The Role of Humic Acid and Biomacromolecules, *Environ. Sci. Technol.*, 2019, **53**, 146–156.

107 E. R. Estes, P. F. Andeer, D. Nordlund, S. D. Wankel and C. M. Hansel, Biogenic manganese oxides as reservoirs of organic carbon and proteins in terrestrial and marine environments, *Geobiology*, 2017, **15**, 158–172.

108 T. N. Tran, D.-G. Kim and S.-O. Ko, Synergistic effects of biogenic manganese oxide and Mn(II)-oxidizing bacterium Pseudomonas putida strain MnB1 on the degradation of 17 α-ethinylestradiol, *J. Hazard. Mater.*, 2018, **344**, 350–359.

109 S. M. Webb, B. M. Tebo and J. R. Bargar, Structural characterization of biogenic Mn oxides produced in seawater by the marine bacillus sp. strain SG-1, *Am. Mineral.*, 2005, **90**, 1342–1357.

110 Y. Cai, K. Yang, C. Qiu, Y. Bi, B. Tian and X. Bi, A Review of Manganese-Oxidizing Bacteria (MnOB): Applications, Future Concerns, and Challenges, *Int. J. Environ. Res. Public Health*, 2023, **20**, 1272.

111 X. Chen, Y. J. Pei, H. Wang, G. J. Wang and S. J. Liao, Removal of Indigo Carmine by Bacterial Biogenic Mn Oxides, *Adv. Mater. Res.*, 2014, **864–867**, 1779–1783.

112 Y.-T. Meng, Y.-M. Zheng, L.-M. Zhang and J.-Z. He, Biogenic Mn oxides for effective adsorption of Cd from aquatic environment, *Environ. Pollut.*, 2009, **157**, 2577–2583.

113 R. Li, L. Zhang, S. Zhu, S. Fu, X. Dong, S. Ida, L. Zhang and L. Guo, Layered δ-MnO2 as an active catalyst for toluene catalytic combustion, *Appl. Catal., A*, 2020, **602**, 117715.

114 P. Shende, P. Kasture and R. S. Gaud, Nanoflowers: the future trend of nanotechnology for multi-applications, *Artif. Cells, Nanomed., Biotechnol.*, 2018, **46**, 413–422.